

Topological Hall signatures of magnetic hopfions

Börge Göbel,^{1,2,*} Collins Ashu Akosa,^{3,4} Gen Tatara,^{3,5} and Ingrid Mertig¹

¹*Institut für Physik, Martin-Luther-Universität Halle-Wittenberg, D-06099 Halle (Saale), Germany*

²*Max-Planck-Institut für Mikrostrukturphysik, D-06120 Halle (Saale), Germany*

³*RIKEN Center for Emergent Matter Science (CEMS), 2-1 Hirosawa, Wako, Saitama 351-0198, Japan*

⁴*Department of Theoretical and Applied Physics, African University of Science and Technology (AUST), Km 10 Airport Road, Galadimawa, Abuja F.C.T, Nigeria*

⁵*RIKEN Cluster for Pioneering Research (CPR), 2-1 Hirosawa, Wako, Saitama, 351-0198 Japan*

(Dated: March 17, 2020)

Magnetic hopfions are topologically protected three-dimensional solitons that are constituted by a tube which exhibits a topologically nontrivial spin texture in the cross-section profile and is closed to a torus. Here, we show that the hopfion's locally uncompensated emergent field leads to a topological Hall signature, although the topological Hall effect vanishes on the global level. The topological Hall signature is switchable by magnetic fields or electric currents and occurs independently of the anomalous and conventional Hall effects. It can therefore be exploited to electrically detect hopfions in experiments and even to distinguish them from other textures like skyrmion tubes. Furthermore, it can potentially be utilized in spintronic devices. Exemplarily, we propose a hopfion-based racetrack data storage device and simulate the electrical detection of the hopfions as carriers of information.

I. INTRODUCTION

Over the recent years, non-collinear spin textures have attracted an enormous research interest. Especially the small whirls called ‘magnetic skyrmions’^{1,2} have outstanding properties which arise from their integer topological charge³

$$N_{\text{Sk}} = \frac{1}{4\pi} \int \mathbf{m}(\mathbf{r}) \cdot \left(\frac{\partial \mathbf{m}(\mathbf{r})}{\partial x} \times \frac{\partial \mathbf{m}(\mathbf{r})}{\partial y} \right) d^2r \quad (1)$$

[$\mathbf{m}(\mathbf{r})$ is the normalized magnetization density]. In nature, the quasi two-dimensional skyrmions elongate as ‘strings’ or ‘tubes’ along the magnetic field direction. For these textures, the occurrence of an additional contribution to the Hall effect of electrons^{4,5} has been observed. Due to the accumulation of a Berry phase upon reorientation of their spin with respect to the locally varying texture, the electrons behave as if they would interact with an emergent magnetic field^{3,6}

$$B_{\text{em},\alpha} = \frac{1}{2} \epsilon_{\alpha\beta\gamma} \mathbf{m}(\mathbf{r}) \cdot \left(\frac{\partial \mathbf{m}(\mathbf{r})}{\partial \beta} \times \frac{\partial \mathbf{m}(\mathbf{r})}{\partial \gamma} \right). \quad (2)$$

This effective field can be gigantic compared to experimentally realizable magnetic fields and it points always along the string direction. The topological Hall effect can in principle be used to electrically detect individual magnetic skyrmions that move in between two leads^{7,8}.

A related object is the magnetic hopfion⁹⁻¹⁴. It can be understood as a skyrmion tube that is closed to a torus [Fig. 1(a)] – this brings about another layer of topological protection, since a torus cannot be transformed to a string continuously. Recently, magnetic hopfions have been stabilized in micro-magnetic simulations¹¹⁻¹³. While considering cross-section textures with higher topological charges or strings that are twisted before forming the closed torus can lead to increased hopf numbers^{15,16}

$$N_H = -\frac{1}{(4\pi)^2} \int \mathbf{B}_{\text{em}}(\mathbf{r}) \cdot \mathbf{A}(\mathbf{r}) d^3r, \quad (3)$$

here, we consider the fundamental hopfions (cf. Fig. 1) characterized by a hopf number of 1, as stabilized in Refs.¹¹⁻¹³. The hopf number is calculated from the texture's emergent field \mathbf{B}_{em} and its corresponding vector potential³⁹, fulfilling $\nabla \times \mathbf{A} = \mathbf{B}_{\text{em}}$.

To be precise, in order to be geometrically compatible with the magnetic surrounding, the cross-section profile of the torus is not a conventional skyrmion but an in-plane skyrmion [cf. Figs. 1(b,c)], also called ‘bimeron’^{17,18}. The texture along every cut that includes the z axis resembles the same two bimerons, but due to the deformation of the string upon forming the torus, the magnetization points along different directions [different colors in the two cuts in Figs. 1(b,c)]. This is also visible in the $z = 0$ cross-section profile in Fig. 1(d) that resembles a Bloch-type skyrmionium – a skyrmion that is positioned in the center of a second skyrmion with mutually reversed spins^{19,20}.

In the following, we calculate the topological contribution to the Hall effect of electrons in different measurement setups by means of Landauer-Büttiker simulations. We find that hopfions exhibit a local topological Hall signature due to a locally uncompensated emergent field, that cancels only on a global level. Based on these findings, we discuss consequences for the electrical detection and for the spintronic applicability of magnetic hopfions.

II. MODEL AND METHODS

We consider a cuboid-shaped region of a cubic lattice, in which the hopfion is located, and add semi-infinite leads attached to the surfaces of the cuboid, in order to simulate currents and charge accumulations. Depending on the measurement geometry, the six leads either cover the whole cuboid or border only parts of it [cf. blue and red detecting leads in Fig. 2(a,c)] to locally probe the topological Hall signature.

For simplicity, we consider a single orbital tight-binding

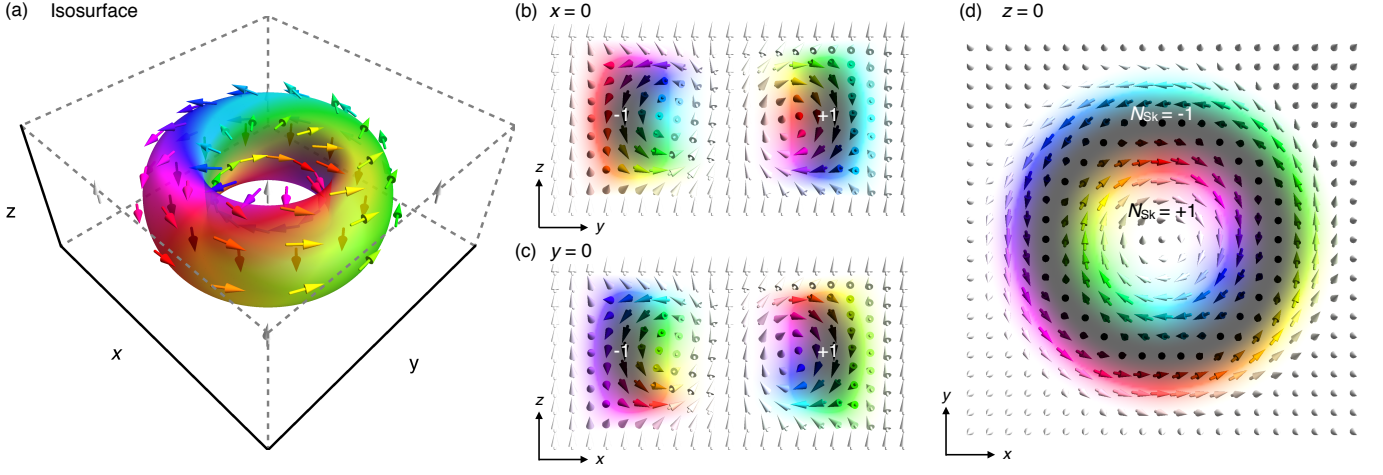


FIG. 1: Magnetic hopfion. In (a) the isosurface $m_z = -0.2$ and selected magnetic moments are shown. In (b,c,d) cuts of the texture at $x = 0$, $y = 0$ and $z = 0$ are shown, respectively. The color represents the in-plane spin orientation. White and black represent $+z$ and $-z$ orientations, respectively. The topological charges of the magnetic objects in these two-dimensional cuts are indicated. These quantities can be related with the emergent field perpendicular to the respective cut (cf. Fig. 3).

model with a hopping term and a Hund's coupling term^{6,21,22}

$$H = t \sum_{\langle i,j \rangle} c_i^\dagger c_j + m \sum_i \mathbf{m}_i \cdot (c_i^\dagger \boldsymbol{\sigma} c_i). \quad (4)$$

Here c_i^\dagger and c_i are the spin-dependent creation and annihilation operators of an electron at lattice site i . The parameter $t = 1$ eV quantifies the nearest-neighbor hopping and m the coupling of electron spins ($\boldsymbol{\sigma}$ vector of Pauli matrices) and the magnetic texture $\{\mathbf{m}_i\}$. If not stated otherwise, we consider the case close to the adiabatic limit, $m = 10t$, where spin parallel and anti-parallel states are separated in energy. The texture for an $N_H = 1$ hopfion is taken from Ref.¹⁰. For a cylindrical region with radius and height L (cylindrical coordinates $\rho = \sqrt{x^2 + y^2}$, polar angle ϕ and height z), the hopfion is described by¹⁰

$$\mathbf{m}(\mathbf{r}) = \begin{pmatrix} \frac{4\Xi\rho(\Omega \cos \phi - (\Lambda-1) \sin \phi)}{(1+\Lambda)^2} \\ \frac{4\Xi\rho(\Omega \sin \phi + (\Lambda-1) \cos \phi)}{(1+\Lambda)^2} \\ 1 - \frac{8\Xi^2\rho^2}{(1+\Lambda)^2} \end{pmatrix}, \quad (5)$$

with

$$\begin{aligned} \Omega &= \tan(\pi z/L), \\ \Xi &= (1 + (2z/L)^2) \sec(\pi\rho/(2L))/L, \\ \Lambda &= \Xi^2\rho^2 + \Omega^2/4. \end{aligned} \quad (6)$$

Outside of this specified region, the magnetization is assumed to point along z .

In a periodic sample, the band structure of such a single orbital model without considering a texture gives a spin degenerate band that ranges from $-6t$ to $+6t$ in energy. Accordingly, in our system, when the coupling to the texture is considered, the density of states is finite for energies between $-m - 6t$ and $+m + 6t$. For $m = 10t$, the relevant energy range is from

-16 eV to 16 eV, with a gap between -4 eV and 4 eV due to the considered strong-coupling limit.

To calculate the Hall resistivity, we use a Landauer-Büttiker method, as presented in Refs.^{8,23} for skyrmions. The six leads i are characterized by currents I_i and voltages U_i that are related by the transmission matrix \underline{T}

$$I_i = \frac{e^2}{h} \sum_j T_{ij} U_j. \quad (7)$$

For the numerical calculation we use the program package Kwant²⁴. The Hall resistance R_{ij} and the Hall angle θ_{ij} are given by

$$R_{ij} = \frac{\Delta U_j}{I_i}, \quad \theta_{ij} = \frac{\Delta U_j}{\Delta U_i}, \quad (8)$$

respectively, with $i, j = x, y, z$ and $i \neq j$.

In general, each Hall resistance tensor element R_{ij} is determined by several contributions. For skyrmionic textures, one typically considers the conventional Hall effect (HE), the anomalous Hall effect (AHE) and the topological Hall effect (THE)^{4,5} of electrons. The conventional Hall effect is proportional to an externally applied magnetic field²⁵ along the perpendicular direction, and the anomalous Hall effect²⁶ arises due to spin-orbit coupling (SOC) and (typically⁴⁰) due to a net magnetization²⁷. The topological Hall resistance is proportional to the average emergent field $\langle B_{em} \rangle$ along the perpendicular direction. This effect arises purely due to the existence of a topologically non-trivial spin texture²⁸, even in the absence of SOC. In order to isolate this fundamental contribution, we do not consider SOC nor an external magnetic field.

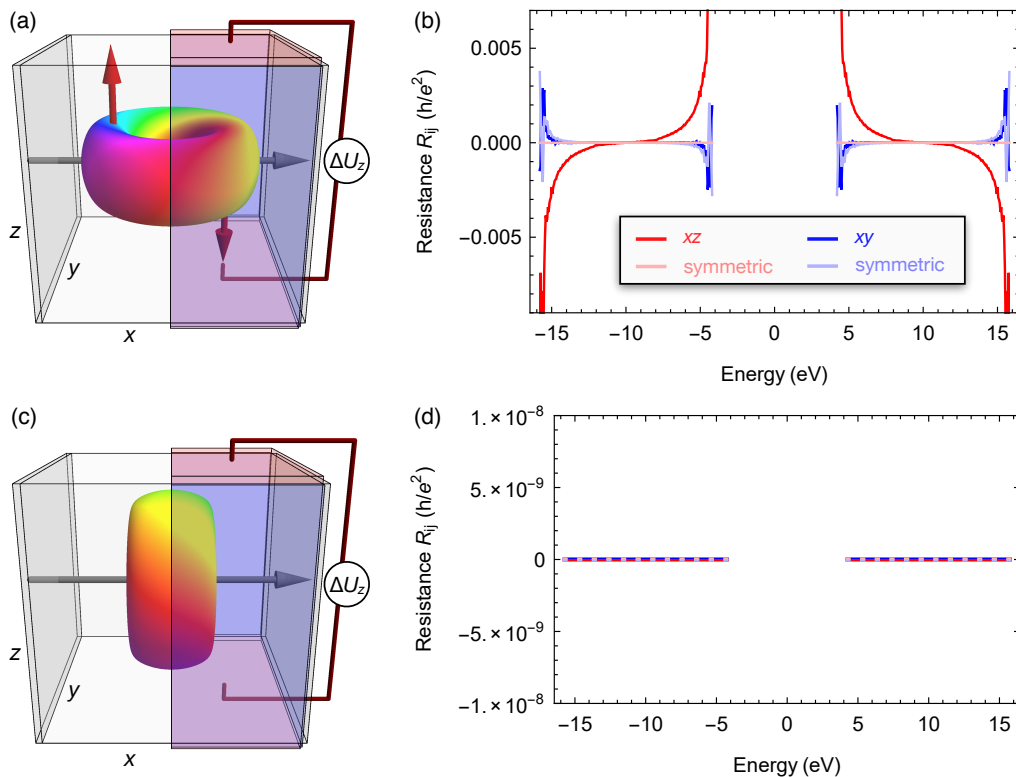


FIG. 2: Topological Hall signal using asymmetric leads. In (a) the hopfion is positioned such that the asymmetrically placed detecting leads (red and blue) enclose one vertically-cut half of the hopfion, so that the average emergent field is pointing along $-y$ (cf. arrows in Fig. 3). The evoked deflection of the current electrons (gray) is indicated by the red arrows. The resulting Hall voltage is detected by the red and blue leads; it gives rise to the corresponding resistance tensor elements shown in (b). The brighter curves show the signal for symmetric leads that cover the whole cube for comparison. In (c,d) the hopfion is reoriented, as indicated.

III. RESULTS AND DISCUSSION

A. Vanishing topological Hall effect on a global level

First, we consider a cube of size $(2L+1) \times (2L+1) \times (2L+1)$ sites with a hopfion in its center (here modeled by $L = 10$). Six leads border the whole cube to simulate a symmetric measurement. We model an applied current along the x direction by adding a small bias voltage $V_{-x} = -V_{+x} = 1$ mV and are interested in the charge accumulation at the other terminals. Therefore, the currents were set to zero $I_{-y} = I_{+y} = I_{-z} = I_{+z} = 0$. Solving Eqs. (7) gives $R_{xz} = 0$ for this geometry⁴¹; cf. light red curve in Figs. 2(b).

This observation can be understood by considering the emergent field of a hopfion (Fig. 3). For the cuts at $x = 0$ and $y = 0$, the spin texture resembles two in-plane skyrmions [Figs. 1(b,c)]. Consequently, the emergent field points along the perpendicular direction, i. e. along the torus. For the cut at $z = 0$ [Figs. 1(d)], the profile is a skyrmionium with a positive out-of-plane emergent field in the center and a negative field for the outer ring. Consequently, the emergent field forms a whirl-like vector field with positive z components in the center and opposite orientations near the hopfion's edge [cf. Fig. 3(b) for better visibility]. The emergent field is characterized by a finite toroidal moment $\mathbf{t} \propto \int \mathbf{r} \times \mathbf{B}_{\text{em}}(\mathbf{r}) d^3r$.

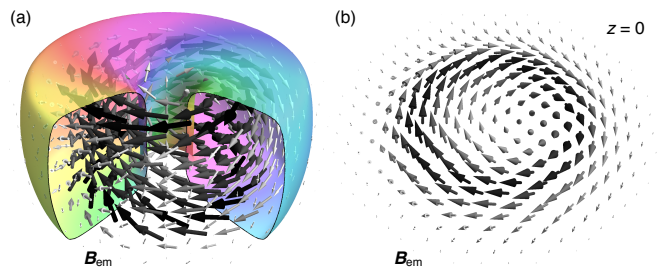


FIG. 3: Emergent field. (a) The arrows visualize the emergent field of a hopfion, where the gray-level represents the magnitude. The colored shell shows a part of the isosurface for $m_z = 0.75$ for the purpose of better visibility. In (b) a cut at $z = 0$ is shown.

The field vanishes on average, and even on a discrete lattice its average in-plane component vanishes perfectly by symmetry explaining $R_{xz} = 0$.

The other resistance tensor element, R_{xy} , is negligible for most energies as well [light blue curve in Fig. 2(b)]. However, finite values occur close to the band edge which originate from the discrete lattice and the small hopfion size⁴². All in all, a hopfion does not exhibit a considerable Hall response in a global measurement.

B. Local topological Hall signature

Even though a globally vanishing emergent field leads to a compensated signal for symmetrically placed leads, the emergent field does not vanish locally. For this reason, in a second simulation, we apply asymmetric leads with respect to the hopfions's center. As shown in Figs. 2(a,c), the leads parallel to the xy and xz planes are only L sites wide and cover only one half of the cube. Consequently, the emergent field in the volume between those leads predominantly determines the magnitude of the topological Hall resistance. Here, the field points along $-y$ on average.

This time, a pronounced R_{xz} signature is observed [red curve in Fig. 2(b)], in agreement with the phenomenological Lorentz-force argument: the force points along $-z$ for an average emergent field along $-y$ and a current along x . Consequently, the applied current (gray) is deflected along $-z$ (red arrow). The hopfion exhibits a considerable local topological Hall effect, with Hall angles of up to 6% (shown in Fig. S1 in the Supplemental Material²⁹). Likewise, if the contacts are attached at the other half of the cube, the sign of R_{xz} is reversed – both contributions cancel in a global measurement.

The sign of the R_{xz} signal is energy dependent and determined by the carrier character and the local spin alignment with respect to the texture. Therefore, it changes comparing the positive and negative energy states (parallel vs. anti-parallel spin alignment), and at the energies $\pm m = \pm 10$ eV, where the predominant carrier concentrations changes from electronic to hole-like, similar to Ref.²¹.

In another simulation, we rotated the hopfion as shown in Fig. 2(c)]. In this configuration, the relevant emergent field vanishes on average, which is why the numerical simulations return vanishing Hall coefficients [Fig. 2(d)].

Following from our results, hopfions can even be distinguished from skyrmion strings in a sample which is magnetized along z : For skyrmions, the Hall response is limited to the xy resistance tensor element. The xz element is zero since the emergent field of a skyrmion string points always along z . Another noteworthy property that can be concluded from these results is that for a hopfion the predominant topological Hall voltage arises parallel to the net magnetization and the stabilizing magnetic field; the R_{xz} tensor element is non-zero. Therefore, if a current is applied within the hopfion plane, as in Fig. 2(a), this particular locally detected topological Hall signal is not superimposed by the anomalous Hall effect and the conventional Hall effect that both have only finite xy elements. This makes hopfions unique and allows for a pure detection of the topological Hall effect.

The above findings are not restricted to the adiabatic limit. A local topological Hall signature arises even for a weak coupling of electron spins and the magnetic texture ($m = 2/3t$ in Fig. S2 in the Supplemental Material²⁹), even though the validity of the emergent field interpretation is limited in that case.

C. Hopfion-based racetrack storage device

A potential spintronic device that can exploit the locally occurring topological Hall effect is a hopfion-based racetrack data storage. Similar to the initially proposed racetracks based on domain walls^{30–32} or the later proposed racetracks based on skyrmions³³, a hopfion-based racetrack is a nano-stripe, where the bits of information are encoded by the presence or absence of hopfions at specific positions. Therefore, the hopfions need to be written, deleted, moved and read. Recently, the current-driven motion of hopfions by spin-transfer and spin-orbit torques has been simulated¹³. The hopfions, that are oriented in the xy plane, move along the track, without any transverse deflection, like in Fig. 4(a). This is highly desirable for a racetrack storage device and can be considered a great advantage for the applicability of hopfions compared to skyrmions. Our finding provides a method to detect the bits in such a geometry by adding detecting leads, similar to the case of skyrmions presented in Refs.^{7,8}; cf. Fig. 4(a). However, here, the leads are positioned perpendicular to z (red).

As expected from our prior findings, the calculated signal R_{xz} [Fig. 4(b)] is antisymmetric with respect to the hopfion displacement $\Delta x = 0$ and exhibits two significant peaks when the hopfion is displaced by approximately $\Delta x = \pm 0.4L$. In these cases, the space-dependent emergent field between the leads

$$\langle \mathbf{B}_{\text{em}} \rangle = \int_{x=-L/4}^{L/4} \int_{y=-L}^L \int_{z=-L/2}^{L/2} \mathbf{B}_{\text{em}}(\mathbf{r} - \Delta\mathbf{r}) d\mathbf{r}$$

(blue dashed curve) has its extremum as well. The relevant emergent field points along $\pm y$, respectively. The good agreement of both curves implies that the Hall resistance is proportional to the relevant emergent field, like in Ref.³⁴.

For a more realistic simulation, we considered also disorder by adding site-dependent random on-site energies that range between $-t/2$ and $+t/2$ ³⁵, which corresponds to a mean free path of 128 lattice constants. An average over 600 impurity configurations has been taken. The calculated signal still features two antisymmetric peaks, even though disorder decreases their magnitudes [cf. orange curve in Fig. 4(b)]. The R_{xz} signal is robust compared to the finite-size mediated R_{xy} that decreases by more than 60% when disorder is taken into account (cf. Fig. S3 in the Supplemental Material²⁹).

IV. CONCLUSION

In summary, we have shown that magnetic hopfions exhibit a local topological Hall signature which is compensated on a global level. As long as the applied current is not perpendicular to the hopfion plane, the toroidal emergent field of the hopfion leads to a local deflection of electrons along the out-of-plane direction. This direction coincides with the net magnetization of a hopfion host and the stabilizing magnetic field. Consequently, this topological Hall signature is expected to be detectable in a pure manner, i. e., without anomalous or conventional Hall effects. It allows to detect hopfions in experiments and to distinguish them from skyrmion strings.

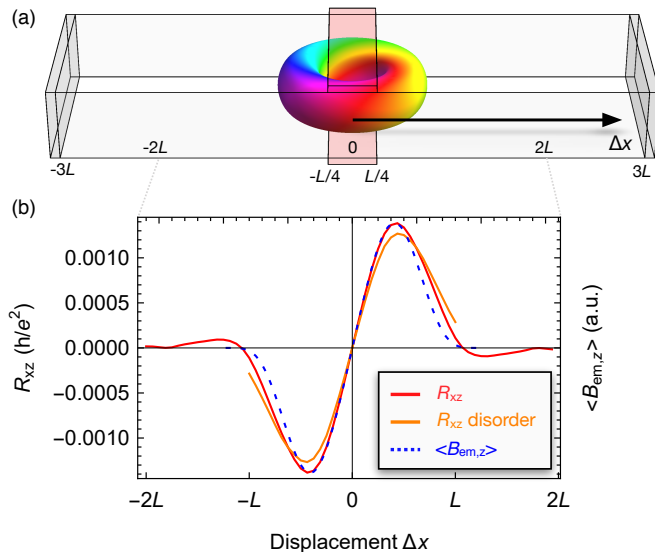


FIG. 4: Local detection of hopfions in a nano-stripe. In (a) the considered geometry is shown with the displacement Δx of the hopfion with respect to the detecting leads, as indicated. A current, flowing between the gray contacts (along x), leads to a Hall voltage between the two red contacts (along $\pm z$). Panel (b) shows the calculated Hall resistance signal (red). For the orange curve, disorder has been taken into account (see main text). The average emergent field between the two red leads is shown as a blue, dashed curve. The simulated racetrack has the dimension: $(6L + 1) \times (2L + 1) \times (L + 1)$ sites, here $L = 16$ sites, which allows to simulate displacements between $-2L$ and $+2L$. The red leads have a width of 9 sites and the Fermi energy is $E_F = -14.0$ eV.

This fundamental finding can be utilized in spintronic de-

vices. Exemplarily, we have discussed a racetrack storage device. Here, the hopfion is a highly promising carrier of information, since its globally compensated emergent field leads to the absence of a skyrmion Hall effect. Therefore, our work does not only contribute to the fundamental understanding of three-dimensional magnetic solitons but opens also avenues towards the realization of innately three-dimensional spintronic applications.

Furthermore, we have shown that the local topological Hall signature depends on the hopfion's orientation, which in micromagnetic simulations is controlled by the stabilizing magnetic field. For this reason, electrical currents can be controlled by tilting an external field. Conversely, if hopfions were found to be stable without magnetic fields in different samples, our results imply that the application of an electrical current would lead to a reorientation of the hopfion: By analogy with skyrmionic systems, a topological Hall effect is accompanied by a torque that manipulates the texture itself. Without a stabilizing field, the application of a current in the setup of Fig. 2(a) would rotate the hopfion to the state in Fig. 2(c), since the torque would have opposite signs for the two sides of the hopfion⁴³. As long as a considerable stabilizing field is present, this effect is however suppressed⁴⁴.

Acknowledgments

This work is supported by TRR 227 of Deutsche Forschungsgemeinschaft (DFG). C. A. A. and G. T. acknowledge support by Grant-in-Aid for Exploratory Research (No. 16K13853) and Grant-in-Aid for Scientific Research (B) (No. 17H02929) from Japan Society for the Promotion of Science (JSPS).

* Corresponding author. boerge.goebel@physik.uni-halle.de

¹ A. Bogdanov and D. Yablonskii, Zh. Eksp. Teor. Fiz **95**, 182 (1989).

² S. Mühlbauer, B. Binz, F. Jonietz, C. Pfleiderer, A. Rosch, A. Neubauer, R. Georgii, and P. Böni, Science **323**, 915 (2009).

³ N. Nagaosa and Y. Tokura, Nature Nanotechnology **8**, 899 (2013).

⁴ A. Neubauer, C. Pfleiderer, B. Binz, A. Rosch, R. Ritz, P. Niklowitz, and P. Böni, Phys. Rev. Lett. **102**, 186602 (2009).

⁵ M. Lee, W. Kang, Y. Onose, Y. Tokura, and N. Ong, Phys. Rev. Lett. **102**, 186601 (2009).

⁶ K. Hamamoto, M. Ezawa, and N. Nagaosa, Phys. Rev. B **92**, 115417 (2015).

⁷ D. Maccariello, W. Legrand, N. Reyren, K. Garcia, K. Bouzehouane, S. Collin, V. Cros, and A. Fert, Nature Nanotechnology **13**, 233 (2018).

⁸ K. Hamamoto, M. Ezawa, and N. Nagaosa, Applied Physics Letters **108**, 112401 (2016).

⁹ P. Sutcliffe, Physical Review B **76**, 184439 (2007).

¹⁰ P. Sutcliffe, Journal of Physics A: Mathematical and Theoretical **51**, 375401 (2018).

¹¹ Y. Liu, R. K. Lake, and J. Zang, Physical Review B **98**, 174437 (2018).

¹² J.-S. B. Tai, I. I. Smalyukh, et al., Phys. Rev. Lett. **121**, 187201 (2018).

¹³ X. Wang, A. Qaiumzadeh, and A. Brataas, Physical Review Letters **123**, 147203 (2019).

¹⁴ F. N. Rybakov, N. S. Kiselev, A. B. Borisov, L. Döring, C. Melcher, and S. Blügel, arXiv preprint arXiv:1904.00250 (2019).

¹⁵ J. Whitehead, Proceedings of the National Academy of Sciences of the United States of America **33**, 117 (1947).

¹⁶ F. Wilczek and A. Zee, Phys. Rev. Lett. **51**, 2250 (1983).

¹⁷ Y. Kharkov, O. Sushkov, and M. Mostovoy, Phys. Rev. Lett. **119**, 207201 (2017).

¹⁸ B. Göbel, A. Mook, J. Henk, I. Mertig, and O. A. Tretiakov, Phys. Rev. B **99**, 060407 (2019).

¹⁹ A. Bogdanov and A. Hubert, Journal of Magnetism and Magnetic Materials **195**, 182 (1999).

²⁰ S. Zhang, F. Kronast, G. van der Laan, and T. Hesjedal, Nano Letters **18**, 1057 (2018).

²¹ B. Göbel, A. Mook, J. Henk, and I. Mertig, Phys. Rev. B **95**, 094413 (2017).

²² B. Göbel, A. Mook, J. Henk, and I. Mertig, New J. Phys. **19**, 063042 (2017).

²³ G. Yin, Y. Liu, Y. Barlas, J. Zang, and R. K. Lake, Phys. Rev. B **92**, 024411 (2015).

²⁴ C. W. Groth, M. Wimmer, A. R. Akhmerov, and X. Waintal, New Journal of Physics **16**, 063065 (2014).

- ²⁵ E. H. Hall, *American Journal of Mathematics* **2**, 287 (1879).
- ²⁶ E. H. Hall, *The London, Edinburgh, and Dublin Philosophical Magazine and Journal of Science* **12**, 157 (1881).
- ²⁷ N. Nagaosa, J. Sinova, S. Onoda, A. MacDonald, and N. Ong, *Rev. Mod. Phys.* **82**, 1539 (2010).
- ²⁸ P. Bruno, V. Dugaev, and M. Taillefumier, *Phys. Rev. Lett.* **93**, 096806 (2004).
- ²⁹ See Supplemental Material [URL will be inserted by publisher] for supplementary figures on the topological Hall angle of electrons in hopfion spin textures, on the topological Hall resistance in the weak-coupling regime, and on the robustness of the considered topological Hall resistance in racetracks compared to other measurement geometries.
- ³⁰ S. S. P. Parkin, *Shiftable magnetic shift register and method of using the same* (2004), US Patent 6,834,005.
- ³¹ S. S. P. Parkin, M. Hayashi, and L. Thomas, *Science* **320**, 190 (2008).
- ³² S. S. P. Parkin and S.-H. Yang, *Nature Nanotechnology* **10**, 195 (2015).
- ³³ J. Sampaio, V. Cros, S. Rohart, A. Thiaville, and A. Fert, *Nature Nanotechnology* **8**, 839 (2013).
- ³⁴ B. Göbel, A. Schäffer, J. Berakdar, I. Mertig, and S. Parkin, *Scientific Reports* **9**, 12119 (2019).
- ³⁵ P. B. Ndiaye, C. A. Akosa, and A. Manchon, *Phys. Rev. B* **95**, 064426 (2017).
- ³⁶ H. Chen, Q. Niu, and A. H. MacDonald, *Phys. Rev. Lett.* **112**, 017205 (2014).
- ³⁷ S. Nakatsuji, N. Kiyohara, and T. Higo, *Nature* **527**, 212 (2015).
- ³⁸ A. K. Nayak, J. E. Fischer, Y. Sun, B. Yan, J. Karel, A. C. Komarek, C. Shekhar, N. Kumar, W. Schnelle, J. Kübler, et al., *Science Advances* **2**, e1501870 (2016).
- ³⁹ The vector potential can be constructed directly from the emergent field in terms of elementary integrals, as shown in Ref.¹⁴.
- ⁴⁰ There are recent reports that also coplanar textures without a net magnetization can exhibit an anomalous Hall effect³⁶⁻³⁸.
- ⁴¹ The calculated values are within the order of magnitude of the numerical precision.
- ⁴² A large angle between two neighbored magnetic moments effectively leads to a decrease of the hopping amplitude. Consequently, for energies near the band edge, the electrons are located predominantly in areas with smaller angles between neighbored spins⁸. The electrons effectively feel a small emergent field which is oriented out of the hopfion plane and causes a finite R_{xy} signal.
- ⁴³ By analogy with the local topological Hall effect of electrons, the two sides of the hopfion would move oppositely to the red arrows in Fig. 2(a).
- ⁴⁴ For example, in the simulations of Ref.¹³ the effect was not observed. Furthermore, even for very small stabilizing fields for which the competition of forces could lead to an intermediate orientation of the hopfion between Figs. 2(a) and (c), the hopfion would rotate back to the initial configuration once the current is tuned off again.